Dynamic structure factors and neutron scattering spectra of liquid ^{3}He-^{4}He mixtures

A. Szprynger
Institute of Low Temperature and Structure Research, Polish Academy of Sciences, P.O. Box 937, 50-950 Wroclaw 1, Poland

M. Lücke
Fachrichtung Theoretische Physik, Universität des Saarlandes, D-6600 Saarbrücken, West Germany
(Received 14 May 1985)

The dynamic structure factors $S_{ij}(k,\omega)$ $(i,j=3,4)$ of density fluctuations in mixtures of various ^{3}He concentrations are evaluated at zero temperature for a range of wave numbers k and frequencies ω centered around the ^{4}He roton excitations. The calculations are performed within a model that has been derived earlier by the authors and which is based upon a 2×2 matrix dispersion-relation representation of the dynamic density susceptibilities of the mixture. The role that the three different partial density-fluctuation spectra $S_{ij}(k,\omega)$ play in determining the spectral structure (and its variation with wave number and concentration) of the total neutron scattering law of the mixture is elucidated in quantitative detail. The theoretical predictions for the latter are compared, after appropriate resolution broadening, with low-temperature experimental neutron scattering spectra obtained for wave-number transfers in the roton range.

I. INTRODUCTION

The dynamical properties of density fluctuations in a mixture of ^{3}He and ^{4}He atoms, i.e., a many-body system consisting of interacting fermions and bosons, represent an interesting and challenging problem.

Historically, the first research efforts[1–9] aimed at determining the dispersion[10] $\epsilon_3(k)$ of ^{3}He quasiparticles in the He II bath. In particular, ^{3}He quasiparticle excitations in the frequency and wave-number range of ^{4}He rotons attracted much interest. Many models were advanced with partly contradictory predictions for the behavior of the dispersion $\epsilon_3(k)$. However, only a few of them[7–9] produced results that are in accord with experimental[11–13] observations: namely a weak monotonic increase of the effective ^{3}He mass with wave number such that $\epsilon_3(k)$ approaches the ^{4}He single-mode dispersion curve $\epsilon_4(k)$ near its roton minimum. The different spectral behavior of ^{3}He excitations below and above the energy-momentum threshold for generation of ^{4}He rotons has been explained by two theories.[8,9]

Also, the change of the ^{4}He single-mode excitation dispersion $\epsilon_4(k)$ induced by ^{3}He impurities was investigated, mainly in the roton vicinity. Since the experimentally observed shifts could not be explained by an approach[14] producing only a dynamical level-repulsion effect between $\epsilon_3(k)$ and $\epsilon_4(k)$, Hilton *et al.*[11] suggested that the increase of the ^{4}He mean particle distances in the presence of ^{3}He atoms might also cause, via a shifted peak in the ^{4}He static structure factor, a change of the ^{4}He excitation energy $\epsilon_4(k)$.

These intuitive, physically plausible arguments were put on firm ground in our theory[15] (hereafter referred to as I). This theory makes use of a 2×2 matrix dispersion representation of the dynamic susceptibilities of the mixture. Approximations to the matrix of self-energies are based on (i) the experimental observation that ^{4}He-roton widths in mixtures[11,16,17] at low temperatures are very small, and (ii) the assumption that the ^{3}He subsystem without the coupling to the ^{4}He bath may be treated as an ideal Fermi gas. We elucidated and showed quantitatively that the altered ^{4}He structure dominates various other static and dynamic effects in determining the energy shift of ^{4}He single-mode excitations in dilute mixtures.[15]

While most of the above theoretical works dealt only with the single-impurity problem or with mixtures of ^{3}He concentration $x=N_3/(N_3+N_4)\leq0.06$, neutron scattering experiments have also been performed on low-temperature ^{3}He-^{4}He mixtures with larger ^{3}He concentrations $x=0.12$ and 0.25. On the other hand, to our knowledge, only one theoretical attempt[18] (to be discussed critically later on in this work) at explaining the larger-x neutron scattering spectra has been reported so far.

In this work we use our theory I, which has already been applied successfully to $x=0.06$ mixtures, to calculate the various density-fluctuation spectra in mixtures with larger ^{3}He concentrations in a broad wave-number band around the roton and compare the results with neutron scattering experiments.

In Sec. II we recall model I. The density-fluctuation spectra of the model are discussed and compared with available experimental data in Sec. III. Possible extensions of the present theory are discussed in the last section.

II. THEORETICAL FRAMEWORK

The neutron scattering intensity from ^{3}He-^{4}He mixtures of ^{3}He concentration x is proportional to[19]

$$S_{\rm tot}(k,\omega)=4.38xS_{33}(k,\omega)+4.07\sqrt{x(1-x)}S_{34}(k,\omega)+(1-x)S_{44}(k,\omega) \quad (2.1)$$

if an incoherent contribution is neglected.

At $T=0$ K the partial dynamic structure factors $S_{ij}(k,\omega)$ are simply related via

$$S_{ij}(k,\omega)=2\Theta(\omega)\mathrm{Im}\chi_{ij}(k,\omega+i0) \tag{2.2}$$

to the imaginary parts of the density-response matrix elements $\chi_{ij}(k,z)$ in terms of which our theory was formulated in I. The theory is based on a matrix dispersion-relation representation of the dynamical 2×2 susceptibility matrix

$$\chi(k,z)=-k^2[z^2-\Omega^2(k)+z\Sigma(k,z)]^{-1}m^{-1}\ . \tag{2.3}$$

Here m is the diagonal matrix of the two bare masses m_3 and m_4, $\Omega_{ij}(k)$ are characteristic frequencies of the restoring forces, and $\Sigma_{ij}(k,z)$ denote the complex self-energies.

Our approximations to the above quantities in I were motivated by the fact that the roton linewidth[11,16,17] is very small, and by the assumption that the ^{3}He subsystem may be described in terms of an ideal Fermi gas (FG). The only damping mechanism for ^{4}He density fluctuations incorporated in our zero-temperature model is the generation of ^{3}He quasiparticle-quasihole excitations.

A. Susceptibilities

With the approximations of I one arrives at the following expressions for the matrix elements $\chi_{ij}(k,z)$. The ^{3}He response function

$$\chi_{33}(,z)=\frac{m^*}{m_3}\frac{\chi_{\mathrm{FG}}(k,z)}{1-V_{\mathrm{eff}}(k,z)\pi_{\mathrm{FG}}(k,z)} \tag{2.4}$$

turns out to be of generalized random-phase-approximation type with the polarization operator $\pi_{\mathrm{FG}}(k,z)$ given in terms of the Lindhard function

$$\pi_{\mathrm{FG}}(k,z)=-\chi_{\mathrm{FG}}(k,z)/\chi_{\mathrm{FG}}(k) \tag{2.5}$$

to be evaluated for an effective mass m^* given below. The effective Fröhlich-like potential

$$V_{\mathrm{eff}}(k,z)=\gamma^2(k)z^2[z^2-\tilde{\epsilon}_4^2(k)]^{-1} \tag{2.6}$$

acting between ^{3}He quasiparticles describes the exchange of virtual ^{4}He excitations of energy

$$\tilde{\epsilon}_4(k)=\epsilon_4(k)[1-W^2(k)]^{-1/2}\ . \tag{2.7}$$

This energy differs from the ^{4}He excitation energy $\epsilon_4(k)$ because ^{3}He and ^{4}He density fluctuations are statically coupled with a strength $W(k)$ to be discussed in Sec. II B. Also, the vertex

$$\gamma(k)=W(k)[1-W^2(k)]^{-1/2} \tag{2.8}$$

is given by $W(k)$. We should like to mention that $\epsilon_4(k)$ is not the single-model energy $\epsilon_4^0(k)$ in pure ^{4}He (hereafter the superscript 0 refers to the $x\to0$ limit), but it is modified according to the altered ^{4}He static structure in the mixture (cf. Sec. II C).

The ^{4}He density-response function reads

$$\chi_{44}(k,z)=\frac{-k^2/m_4}{z^2-\tilde{\epsilon}_4^2(k)[1+\gamma^2(k)\pi(k,z)]}\ . \tag{2.9}$$

The imaginary part of the polarization operator

$$\pi(k,z)=\pi_{\mathrm{FG}}(k,z)[1-\gamma^2(k)\pi_{\mathrm{FG}}(k,z)]^{-1} \tag{2.10a}$$

describes decay into (interacting) ^{3}He quasiparticle-quasihole excitations. Thus, in our model ^{4}He fluctuations with frequency ω and wave number k are damped only in the band

$$k^2/2m^*-kv_F<\omega<k^2/2m^*+kv_F\ , \tag{2.10b}$$

where $\pi''(k,\omega)$ is nonzero.

The cross susceptibility is given by

$$\chi_{34}(k,z)=-\left[\frac{m_3}{m_4}\right]^{1/2}\gamma(k)\chi_{33}(k,z)\frac{\omega_{\mathrm{FG}}(k)\tilde{\epsilon}_4(k)}{z^2-\tilde{\epsilon}_4^2(k)}\ , \tag{2.11}$$

where

$$\omega_{\mathrm{FG}}^2(k)=k^2/[m^*\chi_{\mathrm{FG}}(k)]$$

determines the Fermi-gas restoring force.

B. Coupling function

The coupling function

$$W(k)=\chi_{34}(k)/[\chi_{33}(k)\chi_{44}(k)]^{1/2}$$

is determined by static susceptibilities. Since these are rather poorly known, we approximated the above ratio of static susceptibilities within a generalized Feynman model for the two-component system in terms of the static structure factors $s_{ij}(k)$ of the mixture. This leads to a coupling

$$W(k)\simeq s_{34}(3s_{34}/4+s_{44})[(3s_{33}^2/4+s_{34}^2)\times(3s_{34}^2/4+s_{44}^2)]^{-1/2} \tag{2.12}$$

that is proportional to $s_{34}(k)$ and thus to the square root $(n_3n_4)^{1/2}$ of the mean number densities. Therefore, as a function of concentration, the coupling is extremal for $x=\frac{1}{2}$.

In Fig. 1 we show the vertex $\gamma(k)$ [Eq. (2.8)] which

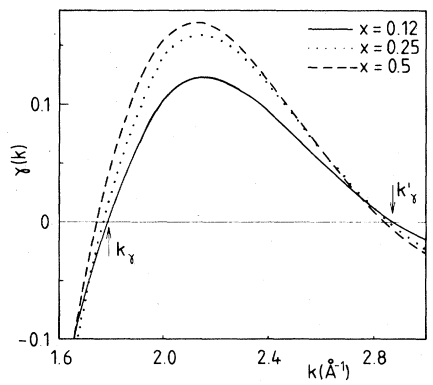

FIG. 1. Vertex $\gamma(k)$, Eq. (2.8), evaluated for three concentrations x with the static structure factors $s_{ij}(k)$ of Ref. 20 as a function of wave number. The wave numbers k_γ and k'_γ, where γ vanishes, are indicated by arrows (shown for the sake of clarity only for $x=0.12$).

practically does not differ from the coupling function $W(k)$ since $W^2(k)$ is less than 0.033 in the wave-number range shown in Fig. 1. To evaluate $W(k)$ [Eq. (2.12)] we used for $s_{ij}(k)$ the results of recent numerical calculations of Fabrocini.[20] Note that the static structure factors $s_{ij}(k)$ cannot be measured separately but only in combination.[21]

The coupling function $W(k)$, and with it the vertex $\gamma(k)$, change sign at wave numbers k_γ and k'_γ, marked in Fig. 1 by arrows for later reference. The change of sign of $W(k)$ is not an artifact of our approximation (2.12); it rather reflects the fact that $\chi_{34}(k)$ is not positive definite.

C. Further input

The structurally induced shift of the ^{4}He single-mode excitation energy in the mixture was approximated in I by

$$\epsilon_4(k)-\epsilon_4^0(k)=\frac{2m_4}{k^2}[\Omega_{44}^0(k)]^2 Z_4^0(k) r_{44}(k) . \quad (2.13)$$

We use for the single-model resonance energy $\epsilon_4^0(k)$, its intensity $Z_4^0(k)$, and the restoring force

$$[\Omega_{44}^0(k)]^2=k^2/[m_4\chi_{44}^0(k)]$$

of pure ^{4}He, the neutron scattering results of Cowley and Woods.[22]

Into Eq. (2.13) enters the relative difference

$$r_{44}(k)=s_{44}^0(k)/s_{44}(k)-1 \quad (2.14)$$

of the ^{4}He static structure factors in the mixture and in pure ^{4}He. To be consistent with the input for the structure factors $s_{ij}(k)$, we use also for the quotient in (2.14) Fabrocini's numerical result.[20]

The function $r_{44}(k)$ is quite similar to the vertex $\gamma(k)$ (Fig. 1). It has two zeros at k_r and k'_r not far from k_γ and k'_γ, respectively, and is positive in between. However, in contrast to k'_γ the momentum k'_r increases with concentration. Moreover, the maximum of the ratio $r_{44}(k)$ grows with x also above $x=0.5$.

Finally, we need the concentration dependence of the momentum-averaged effective mass of ^{3}He. It was obtained from Greywall's measurements[23] at $x=1$ and calculations[9] for $x\to 0$. In the concentration range considered our admittedly crude estimation varied between $m^*=3.3m_3$ and $3.6m_3$.

We should like to note that our results are far less sensitive to an uncertainty of the m^* input than to an uncertainty in the $s_{ij}(k)$ data. The latter enter both the coupling $W(k)$ [Eq. (2.12)] and the structurally induced ^{4}He excitation-energy shift [Eqs. (2.13) and (2.14)]. It would be highly desirable to have more accurate data for the static structure factors in ^{3}He-^{4}He mixtures.

III. RESULTS

A. Dynamic structure factors $S_{ij}(k,\omega)$

The spectral structure of $S_{ij}(k,\omega)$ largely depends on the position of the ^{4}He energy $\tilde{\epsilon}_4(k)$ relative to the band (2.10b) of the ^{3}He quasiparticle-quasihole excitation continuum and on the size of the coupling $\gamma(k)$ (Fig. 1). It is clear from Sec. II A that, in our model, $S_{44}(k,\omega)$ reduces to a δ function, $S_{34}(k,\omega)$ vanishes, and $S_{33}(k,\omega)$ becomes a simple Lindhard function when the coupling $\gamma(k)$ goes to zero for $k\to k_\gamma, k'_\gamma$. In the following we therefore consider wave numbers for which $\gamma(k)\neq 0$.

Before we discuss in more detail the situation in which $\tilde{\epsilon}_4$ lies within the band, which prevails for wave numbers in the roton vicinity, we shall briefly describe the spectra for the other case.

1. $\tilde{\epsilon}_4(k)$ is outside the ^{3}He quasiparticle-quasihole band

In this case $S_{33}(k,\omega)$ is similar to the Lindhard function except for a δ spike close to $\tilde{\epsilon}_4(k)$ of negligible intensity. If the ^{4}He level $\tilde{\epsilon}_4(k)$ lies above the band, then the ^{3}He dispersion $\epsilon_3(k)$ marked by the maximum of $S_{33}(k,\omega)$ is shifted downwards due to the negative real part $\pi'_{\rm FG}$ of the polarization operator. This repulsion of ^{4}He and ^{3}He energy levels increases with increasing $\gamma(k)$ and decreasing distance between the levels. However, in any case $\epsilon_3(k)$ does not differ much from $k^2/2m^*$.

Also, the cross spectrum $S_{34}(k,\omega)$ is a smooth function with the same (opposite) sign as $\gamma(k)$ if $\tilde{\epsilon}_4(k)$ lies above (below) the band.

The ^{4}He spectrum, on the other hand, is dominated by a δ spike at $\omega\approx\tilde{\epsilon}_4$ whenever $\epsilon_4(k)$ lies outside the band—the additional smooth contribution to $S_{44}(k,\omega)$ inside the band is negligible unless $\tilde{\epsilon}_4$ lies very close to a band edge. In that case the peak's side wing inside the band acquires more weight.

2. $\tilde{\epsilon}_4(k)$ is inside the ^{3}He quasiparticle-quasihole band

In Fig. 2 we show, for a concentration of $x=0.25$ as a representative example, the spectra $S_{ij}(k,\omega)$ together with $S_{\rm tot}(k,\omega)$, Eq. (2.1), for two wave numbers for which $\tilde{\epsilon}_4(k)$ lies inside the ^{3}He band. For $k=1.7$ Å^{-1} [Fig. 2(a)] all spectral structures are much sharper than for $k=2.1$ Å^{-1} [Fig. 2(b)] because the vertex $\gamma(k=1.7\text{ Å}^{-1})=-0.066$ is of smaller absolute size than $\gamma(k=2.1\text{ Å}^{-1})=+0.159$. Moreover, $\tilde{\epsilon}_4$ lies closer to the band edge in Fig. 2(a) than in Fig. 2(b).

A striking feature of $S_{33}(k,\omega)$ (dashed line) and $S_{34}(k,\omega)$ (dotted line) is the common zero at $\omega=\tilde{\epsilon}_4(k)$, so we will discuss its origin and consequences. The effective potential (2.6) between ^{3}He quasiparticles that is induced by an exchange of a virtual ^{4}He excitation of energy $\tilde{\epsilon}_4$ forces $S_{33}(k,\omega)$ to be zero at $\tilde{\epsilon}_4(k)$. Consequently, the ^{3}He excitation continuum $S_{33}(k,\omega)$ is split into two parts by a dip the width of which is proportional to the strength $\gamma^2(k)$ [Eq. (2.8)] of the exchange potential. Thus the splitting varies with concentration practically in the same way as $\gamma^2(k)$ or $W^2(k)$: it increases for $x<0.5$ and decreases thereafter.

The cross spectrum $S_{34}(k,\omega)$ Eq. (2.11), changes sign at $\tilde{\epsilon}_4(k)$, and thus shows a positive peak at the low-frequency side of $\tilde{\epsilon}_4(k)$ and a negative peak at the high-frequency side. This behavior holds for $\gamma(k)>0$ as in Fig. 2(b). For $\gamma<0$ [Fig. 2(a)] the peak structure is reversed, with $S_{34}(k,\omega)$ being proportional to $\gamma(k)$. The peaks become

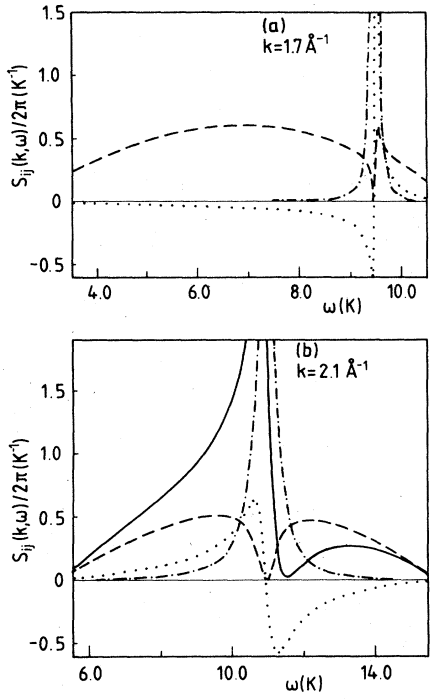

FIG. 2. Density-fluctuation spectra $S_{33}(k,\omega)$ (dashed lines), $S_{34}(k,\omega)$ (dotted lines), $S_{44}(k,\omega)$ (dotted-dashed lines), and $S_{\rm tot}(k,\omega)$ [solid line in (b)] for $x=0.25$. The spectra S_{33} and S_{34} have a common zero at $\omega=\tilde{\epsilon}_4(k)$, Eq. (2.7). See text for a detailed discussion.

sharper when either $\tilde{\epsilon}_4$ approaches the band edge or when the coupling between both subsystems, i.e., $\gamma(k)$, increases.

In the immediate vicinity of the zero at $\tilde{\epsilon}_4(k)$, i.e., for frequencies such that the absolute size of the reduced distance from $\tilde{\epsilon}_4(k)$, $\hat{\omega}=\omega/\tilde{\epsilon}_4(k)-1$, is small compared to unity, the ^{3}He spectrum is approximately quadratic,

$$S_{33}(k,\omega)=a(k)[1+c(k)\hat{\omega}]\hat{\omega}^2 , \tag{3.1}$$

and the cross spectrum is approximately linear in $\hat{\omega}$,

$$S_{34}(k,\omega)=b(k)\{1+[c(k)-\tfrac{1}{2}]\hat{\omega}\}\hat{\omega} . \tag{3.2}$$

The curvature

$$a(k)=8\gamma^{-4}(k)\chi''_{\rm FG}(k,\tilde{\epsilon}_4)m^*/m_3 \tag{3.3a}$$

of the dip of $S_{33}(k,\omega)$ and the slope

$$b(k)=-a(k)\gamma(k)\omega_{\rm FG}(k)\sqrt{3/4} \tag{3.3b}$$

of $S_{34}(k,\omega)$ are rather large because of the inverse powers of the small vertex entering (3.3).

The correction

$$c(k)=4\gamma^{-2}\pi'_{\rm FG}(\tilde{\epsilon}_4)/|\pi_{\rm FG}(\tilde{\epsilon}_4+i0)|^2-3 +\partial\ln[\chi''_{\rm FG}(\tilde{\epsilon}_4)/|\pi_{\rm FG}(\tilde{\epsilon}_4+i0)|^2]/\partial\tilde{\epsilon}_4 \tag{3.4}$$

to the quadratic behavior of (3.1) gives rise to a dip asymmetry in $S_{33}(k,\omega)$. Its largest contribution comes from the first term in (3.4). In the above formula the k dependence is not explicitly displayed. The correction term $[c(k)-\frac{1}{2}]\hat{\omega}$ to the linear behavior of $S_{34}(k,\omega)$, Eq. (3.2), gives rise to a curvature that decreases (increases) the height of the peaks of $S_{34}(k,\omega)$ as long as the correction term is negative (positive). This effect may be seen in Fig. 2(a), where γ^2 is much smaller than in Fig. 2(b).

The position of the higher peak is below (above) $\tilde{\epsilon}_4$ if $\pi'_{\rm FG}(\tilde{\epsilon}_4)$ is negative (positive). As a function of k,

$$\pi'_{\rm FG}(k,\tilde{\epsilon}_4)/|\pi_{\rm FG}(k,\tilde{\epsilon}_4+i0)|^2$$

has a minimum at about $k\approx 2$ Å^{-1}. On the other hand, at fixed momentum it increases monotonously with concentration passing from negative to positive values for $1.85\ \text{Å}^{-1}\lesssim k\lesssim 2.15\ \text{Å}^{-1}$. Thus with growing x a transfer of the spectral weight from one to the other peak may appear. Therefore at $k=2.0$ Å^{-1} the sharper peak is positive for $x=0.12$ and negative for $x=0.5$.

B. Scattering intensity $S_{\rm tot}(k,\omega)$

In Fig. 3 we show the total scattering intensity $S_{\rm tot}(k,\omega)$ [Eq. (2.1)] for three different concentrations and for several wave numbers.

The main peak near $\tilde{\epsilon}_4(k)$ is due to the ^{4}He contribution $S_{44}(k,\omega)$. It should be noted that our theory overesti-

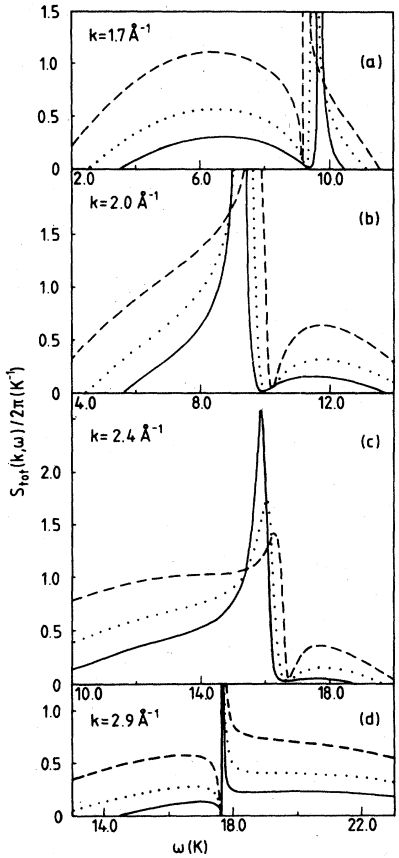

FIG. 3. Total dynamic structure factor $S_{\rm tot}(k,\omega)$ for concentrations $x=0.12$ (solid lines), 0.25 (dotted lines), and 0.5 (dashed lines).

mates the peak height since the total spectral weight of $S_{44}(k,\omega)$ in our single-mode model for the ^{4}He excitation spectrum is practically centered in one peak, whereas in reality it is distributed over the low-lying single-mode excitations and a high-frequency multimode continuum.

With increasing concentration the prefactors in (2.1) depress the ^{4}He contribution to $S_{\rm tot}(k,\omega)$ and enhance those from $S_{33}(k,\omega)$ and $S_{34}(k,\omega)$. This leads to a considerable reduction of the main peak's intensity in $S_{\rm tot}(k,\omega)$, to be seen in Fig. 3. The variation of the main peak's position as a function of concentration is discussed in Sec. III D.

The contribution from the cross spectrum to $S_{\rm tot}(k,\omega)$ causes the main peak to be asymmetric: Its steep falloff is produced mainly by the negative peak of $S_{34}(k,\omega)$. Thus for wave numbers $k_\gamma < k < k'_\gamma$ ($k < k_\gamma$ or $k > k'_\gamma$), where $\gamma(k) > 0$ [$\gamma(k) < 0$], so that the negative part of $S_{34}(k,\omega)$ is located above (below) $\tilde{\epsilon}_4$, the high- (low-) frequency side of the main peak in Figs. 3(b) and 3(c) [Figs. 3(a) and 3(d)] is the steep one. We remark in passing that Pedersen and Cowley[18] obtained a different main-peak asymmetry, which is partly due to the somewhat arbitrary form of their dynamic susceptibility matrix.

Also, the characteristic features of the contribution from $S_{33}(k,\omega)$ (cf. Fig. 2) can easily be recognized in $S_{\rm tot}(k,\omega)$ (Fig. 3). It is the growing bandwidth of the ^{3}He quasiparticle-quasihole continuum with increasing concentration that causes the associated spectral broadening of $S_{\rm tot}(k,\omega)$ as x becomes larger. Note that in the frequency range below (above) the main peak's position where—for $k_\gamma < k < k'_\gamma$ in Figs. 3(b) and 3(c) [for $k < k_\gamma$ and $k > k'_\gamma$ in Figs. 3(a) and 3(b)]—both spectra, S_{33} and S_{34}, are positive, they combine to enhance the spectral weight in $S_{\rm tot}(k,\omega)$ in comparison with the frequency range above (below) the main peak.

Lastly, we should like to mention that the contribution to the total scattering intensity from $S_{34}(k,\omega)$ Is never negligible. It modifies considerably the main peak also for small concentrations.

C. Comparison with experimental scattering spectra

Since the peaks in $S_{\rm tot}(k,\omega)$ (Fig. 3) are strongly asymmetric, one has to be careful when comparing them with resolution-broadened spectra measured in experiments[11] at a fixed scattering angle φ. Therefore, we (i) transformed our $S_{\rm tot}(k,\omega)$ into a constant-scattering-angle spectrum $S_{\rm tot}(\varphi,\omega)$, and (ii) convoluted it with a Gaussian resolution function of half-width 1 K that is appropriate for the experiments of Hilton *et al.*[11] In Fig. 4 the resulting spectra $\bar{S}_{\rm tot}(\varphi,\omega)$ (solid curves) are compared with experimental data[11] for a $x=0.25$ mixture at $T=0.75$ K. The peak positions of $\bar{S}_{\rm tot}(\varphi,\omega)$ correspond to wave numbers (a) $k=1.80$ Å^{-1}, (b) 1.93 Å^{-1}, (c) 2.03 Å^{-1}, and (d) 2.10 Å^{-1}, respectively.

Plotting the spectra at constant scattering angle does not lead to structures that differ from those found at constant-wave-number transfer, but the whole spectrum becomes slightly compressed (e.g., by about 1.5 K at $\varphi=123°$). The convolution with the Gaussian of half-width 1 K, on the other hand, has a bigger effect: First of all, the experimental resolution curve is too broad to let much of the fine structure and the peak asymmetry survive in $\bar{S}_{\rm tot}(\varphi,\omega)$. In fact, the spectra shown in Fig. 4 are all quite similar, and, more importantly, the convolution not only smoothes the original theoretical spectrum $S_{\rm tot}(\varphi,\omega)$ (dashed lines), but also shifts the main peak of $S_{\rm tot}(\varphi,\omega)$ in the direction of its more intensive side wing, that is, for the wave numbers $k_\gamma < k < k'_\gamma$ in Fig. 4, to-

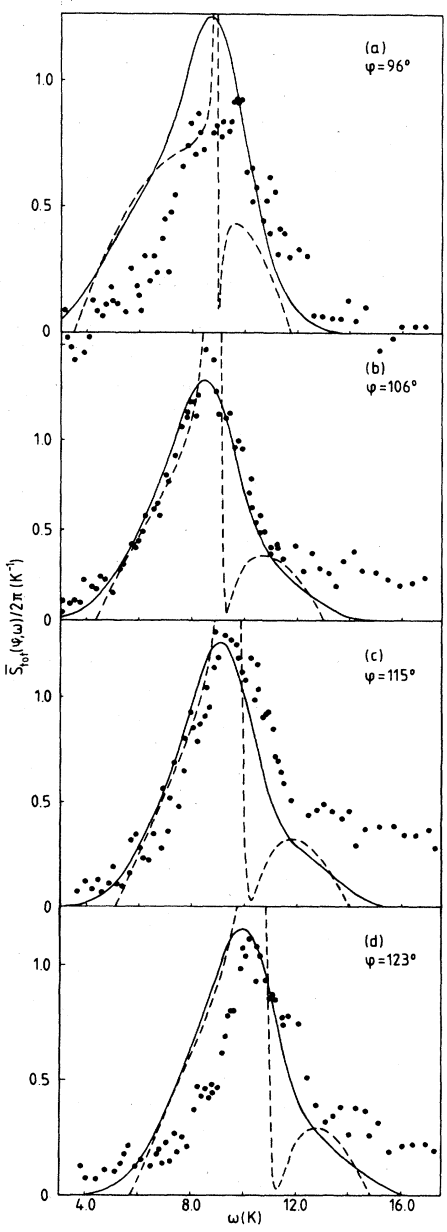

FIG. 4. Dynamic structure factors of the $x=0.25$ mixture for various fixed scattering angles φ. The dashed lines represent the result $S_{\rm tot}(\varphi,\omega)$ of our model. Solid lines show $\bar{S}_{\rm tot}(\varphi,\omega)$, its convolution with a Gaussian of half-width 1 K. Points are neutron scattering data (Ref. 11) measured at $T=0.75$ K. The arbitrary scale factor of the experimental data was fixed at $\varphi=106°$. The peak positions of $\bar{S}_{\rm tot}(\varphi,\omega)$ correspond to wave numbers (a) $k=1.80$, (b) 1.93, (c) 2.03, and (d) 2.10 Å^{-1}.

ward smaller frequencies. For $k<k_\gamma$ or $k>k'_\gamma$, where the main peak's asymmetry is different (cf. Secs. III A and III B), the peak is shifted upward by the convolution.

Note the experimental problem that arises in measuring the change of the main-peak position in the mixture relative to that in pure ^{4}He: Given that the spectrum of the former (latter) *before* resolution broadening is asymmetric (symmetric) near the peak, and given that the experimental resolution curve in the mixture is wider than in pure ^{4}He, one cannot measure the ^{3}He-induced peak shift without a theoretical model that gives the peak asymmetry in the mixture.

The experimental spectra in Figs. 4(b)—4(d) show a marked high-frequency background which our $S_{\rm tot}(\varphi,\omega)$ fails to reproduce fully. One reason could be that, since the high-frequency hump in $S_{\rm tot}(\varphi,\omega)$ (dashed curve) is caused by the contribution $S_{33}(k,\omega)$, the former is cut off in our model at the upper band edge of the ^{3}He quasiparticle-quasihole continuum, while in reality $S_{33}(k,\omega)$ extends to higher frequencies. An additional second reason could be that our spectrum $S_{44}(k,\omega)$ does not contain high-frequency multimode excitations of ^{4}He density fluctuations.

Note, however, that for $\varphi=90°$ the experimental spectrum in Fig. 4(a) does not display a high-frequency background, but is rather well described on the high-frequency side by our model, which does not contain spectral intensities at frequencies above the quasiparticle-quasihole band.

D. Position of the main peak in $S_{\rm tot}(k,\omega)$

The dispersion curve determined by the main peak positions in $S_{\rm tot}(k,\omega)$ differs from $\epsilon_4^0(k)$ due to four effects, of which the altered ^{4}He structure (e.g., the altered mean distance between ^{4}He atoms) in the mixtures is the most important (cf. I for more details).

The structural change causes, via $r_{44}(k)$, Eq. (2.14), a shift (2.13) of the ^{4}He single-mode excitation energy. This shift is positive in the wave-number range $k_r<k<k'_r$, where $r_{44}(k)>0$ and is negative outside this interval. The size of the shift increases with concentration. At $k\simeq 2.2$ Å^{-1}, where this structurally induced energy shift is maximal with respect to wave numbers, its values are 0.64 K for $x=0.12$ and 1.39 K or $x=0.5$.

A second effect is that the coupling (2.12) to the ^{3}He system increases the ^{4}He single-mode fluctuation frequency $\epsilon_4(k)$ to $\tilde{\epsilon}_4(k)$, Eq. (2.7), by about 10%. At $k=2.2$ Å^{-1}, for example, this amounts to an energy shift of 0.09 K at $x=0.12$ and 0.14 K at $x=0.5$.

The third effect is a level repulsion between ^{3}He excitation energies centered around $k^2/2m^*$ and the ^{4}He energy level at $\tilde{\epsilon}_4(k)$. This renormalization of ^{4}He excitation energies is produced by the real part of the polarization operator π [Eq. (2.10a)] that describes the *dynamic* interaction between the two subsystems generated by decay of ^{4}He density fluctuations into ^{3}He quasiparticle-quasihole excitations. However, since the vertex strength $\gamma^2(k)$ multiplying π in (2.9) is rather small, the level repulsion is, at its maximum, $k=2.3$ Å^{-1}, only 0.08 K for $x=0.12$ and 0.14 K for $x=0.5$.

The fourth mechanism is the contribution of the cross spectrum $S_{34}(k,\omega)$ that shifts the peak of $S_{\rm tot}(k,\omega)$ toward the frequencies for which $S_{34}(k,\omega)>0$. Thus this effect lowers (raises) the main peak's frequency in the wave-number range $k_\gamma<k<k'_\gamma$ ($k<k_\gamma$ and $k>k'_\gamma$). Note that the sign of this peak shift differs from that resulting from a model of Pedersen and Cowley,[18] which is discussed in more detail below. The maximum of this effect occurs in our model at $k=2.2$ Å^{-1}, where it yields a downward shift of -0.11 K at $x=0.12$ and of -0.44 K at $x=0.5$.

The combination of all four effects described above combined yields a shift of the peak frequency of $S_{\rm tot}(k,\omega)$ in the mixture relative to the single-model excitation energy $\epsilon_4^0(k)$ of pure ^{4}He that is maximal at $k=2.2$ Å^{-1} and upwards of 0.64 K in size for $x=0.12$, 0.84 K for $x=0.25$, and 1.23 K for $x=0.5$. For the last concentration, $S_{\rm tot}(k,\omega)$ shows only a weak maximum. These effective shifts are dominated by the first effect, namely the structurally induced change of the ^{4}He single-mode excitation energy. Also, the wave numbers for which the effective total shift vanishes coincide practically with k_r and k'_r, where $r_{44}(k)=0$, i.e., where the static structure functions $s_{44}(k)$ and $s_{44}^0(k)$ intersect.

We have already discussed in Sec. III C that the peak positions of the resolution-broadened neutron scattering spectra of Fig. 4 do not allow extraction of the above-described peak shifts of $S_{\rm tot}(k,\omega)$ relative to $\epsilon_4^0(k)$ since the "real" spectra *before* resolution broadening are strongly asymmetric. Therefore one has to convolute any theoretical spectra with the experimental resolution curve and then compare the resulting peak position with the experimental one. Doing this we find semiquantitative agreement with the neutron scattering results of Hilton *et al.*[11]

Finally, we would like to comment on the theory of density excitations in ^{3}He-^{4}He mixtures proposed recently by Pedersen and Cowley.[18] This approach, based on the polarization potentials of Aldrich and Pines,[24] does not make explicit use of the static structure factors $s_{ij}(k)$, so in this theory it is difficult to identify the structural effects mainly responsible for e.g., the roton energy shift in the mixture.

Instead, the authors, by choosing rather arbitrarily the sign of their cross spectrum $S_{34}(k,\omega)$ [it yields a positive $s_{34}(k)$ for wave numbers in the phonon region], suggested that it is just this spectrum which causes the experimentally observed behavior: the negative (positive) peak shift for smaller (larger) wave numbers. As we have shown, such an explanation, which ignores the dominant structural effect, is wrong. Presumably, their misconception is due to the fact that $S_{34}(k,\omega)$ changes its shape more or less accidentally around the wave number where the peak shift (caused mainly by other effects) changes sign.

We have evaluated their $S_{44}(k,\omega)$ (for $k=1.8$ and 2.0 Å^{-1} and $x=0.5$) and found that its peaks are shifted with respect to pure ^{4}He, and that it is this spectrum which practically determines the dispersion of the peak position in the mixture. It might be interesting to see whether the peak shift of their $S_{44}(k,\omega)$ can be identified

as a structural effect hidden in their polarization potentials.

As a final point their theory is, at least at small concentrations, in conflict with the level repulsion between ^{3}He quasiparticles and ^{4}He phonon-roton excitations, since their ^{3}He effective mass decreases with increasing wave numbers. On the other hand, an advantage of their approach is that the ^{3}He dynamic susceptibility is also suitable for the high-concentration limit $x \to 1$, which is not accessible in our model in its present form.

E. Half-width of the main peak in $S_{\rm tot}(k,\omega)$

The only ^{4}He excitation damping of our model is due to the decay into a continuum of ^{3}He quasiparticle-quasihole excitations. We discuss first the half-width $\Gamma_{44}(k)$ of the peak in $S_{44}(k,\omega)$. Approximating it by a Lorentzian, we find from (2.9) and (2.10a), with $\gamma^2 \ll 1$, that

$$\Gamma_{44}(k) \approx \frac{\gamma^2(k)}{2} \tilde{\epsilon}_4(k) \, | \, \pi''_{\rm FG}(k,\tilde{\epsilon}_4) \, | \ . \tag{3.5}$$

Two principal effects determine $\Gamma_{44}(k)$: the ^{3}He phase space $| \, \pi''_{\rm FG}(k,\tilde{\epsilon}_4) \, |$ accessible for the decay, and the strength $\gamma^2(k)$. The latter increases with growing concentration, whereas $| \, \pi''_{\rm FG} \, |$ decreases because the maximum of $\chi''_{\rm FG}(k,\omega)$ at $\omega = k^2/2m^*$ is proportional to k_F^{-1}, and the static susceptibility $\chi_{\rm FG}(k)$ increases in the k range considered here. Moreover, $| \, \pi''_{\rm FG}(k,\tilde{\epsilon}_4) \, |$ can decrease when the distance between $\tilde{\epsilon}_4(k)$ and the band edge at $k^2/2m^* + kv_F$ decreases with growing x.

The wave-number dependence of $\Gamma_{44}(k)$ can be described as follows. The resonance position enters the band at a wave number $k < k_\gamma$, so that $\Gamma_{44}(k)$ initially grows with k over a short interval and then decreases again to zero at k_γ, where the vanishing vertex produces a δ spike in $S_{44}(k,\omega)$. Then for $k_\gamma < k < k'_\gamma$, where $\gamma(k) > 0$, the half-width increases, reaching its maximum at 2.2 Å^{-1}: 0.20 K for $x = 0.06$, 0.29 K for $x = 0.12$, 0.39 K for $x = 0.25$, and 0.32 K for $x = 0.5$.

The width of the main peak in $S_{\rm tot}(k,\omega)$ is not determined by $\Gamma_{44}(k)$ alone, but rather is strongly influenced by $S_{33}(k,\omega)$ as well. Since the peak width of $S_{44}(k,\omega)$ fits into the dip of $S_{33}(k,\omega)$, the combination spectrum $S_{\rm tot}(k,\omega)$ is substantially broadened in comparison with $S_{44}(k,\omega)$. With increasing x the relative weight of the $S_{33}(k,\omega)$ contribution increases and the well-defined ^{4}He resonances in $S_{\rm tot}(k,\omega)$ disappear altogether. The half-width of the main peak $\Gamma_{\rm tot}(k)$ is maximal at $k = 2.2$ Å^{-1} in our model, with the values 0.2 K for $x = 0.06$, 0.40 K for $x = 0.12$, and 0.80 K for $x = 0.25$.

Also, the width of the main peak of the dynamic structure factor $\bar{S}_{\rm tot}(k,\omega)$ (broadened by the Gaussian resolution function of half-width 1 K) increases linearly with concentration. The slope of the increase is quite close to the experimentally[11] observed value, 4 K.

Let us note that the measured half-width in the $x = 0.06$ mixture shows as a function of wave number an evident enhancement when the ^{4}He resonance position enters the quasiparticle-quasihole band and a decrease immediately afterwards, when k approaches k_γ. As a possible explanation of such a behavior, we suggest the weakening of the coupling $\gamma(k)$ between ^{3}He and ^{4}He fluctuations for $k \to k_\gamma$.

IV. FINAL REMARKS

Here we discuss possible extensions of our theory, e.g., to wave numbers and frequencies further away from the roton vicinity.

In our model's present form the ^{4}He subsystem contains (if the coupling γ to the ^{3}He system is switched off) only undamped single-mode excitations as a result of effectively approximating the self-energy $\Sigma_{44}(k,z)$ in (2.3) by a frequency-independent real part. Thus the (decay) coupling to ^{4}He multimode excitations, relevant at larger frequencies, should be incorporated there. Also (decay into) mixed ^{3}He-^{4}He fluctuations $\sim \rho_3(\mathbf{k},t)\rho_4(\mathbf{k}-\mathbf{q},t)$ have been ignored so far in $\Sigma_{44}(k,z)$ and $\Sigma_{33}(k,z)$. These multimode processes also give rise to damping outside the quasiparticle-quasihole frequency band. Furthermore, since our $\Sigma_{33}(k,z)$ was approximated by the self-energy of the ideal Fermi gas of mass m^*, one could take a more realistic self-energy, e.g., from recent theoretical works.[25]

In addition, one might want to include the off-diagonal self-energies $\Sigma_{34}(k,z)$ in the dispersion-relation representation (2.3). A possible way of doing this was presented in Appendix C of I. However, we think that the main coupling between ^{4}He roton excitations and ^{3}He quasiparticles does not come from Σ_{34}, but rather from the off-diagonal terms of the restoring forces $\Omega_{34}(k)$, and that Σ_{34} contains only additional processes like, e.g., coupling of multimode excitations. We should like to emphasize once again that, within the 2×2 matrix representation (2.3) of the susceptibilities, it is the coupling $W(k)$ produced by $\Omega_{34}(k)$ which leads in the ^{4}He response function (2.9) to a polarization operator of which the imaginary part describes decay of ^{4}He fluctuations into ^{3}He quasiparticle-quasihole excitations (cf. I for a detailed discussion).

Therefore we expect the results of the present theory to be changed outside the quasiparticle-quasihole band, but since in the roton vicinity the ^{4}He excitations are relatively sharp, and since the approximation of the ^{3}He subsystem by an ideal Fermi gas seems to be reasonably realistic, we think that there our present results will not be altered substantially by the above-discussed effects.

ACKNOWLEDGMENTS

We wish to thank Professor A. Fabrocini for supplying us with his numerical results prior to publication. One of us (A.S.) acknowledges the hospitality of the Universität des Saarlandes, where most of this work was done.

[1] L. D. Landau and I. Ya. Pomeranchuk, Dokl. Akad. Nauk **59**, 669 (1948); I. Ya. Pomeranchuk, Zh. Eksp. Teor. Fiz. **19**, 42 (1949).

[2] L. P. Pitaevskij (private communication).

[3] V. I. Sobolev and B. Esel'son, Zh. Eksp. Teor. Fiz. Pis'ma Red. **18**, 689 (1973).

[4] C. M. Varma, Phys. Lett. **45A**, 301 (1973).

[5] M. J. Stephen and L. Mittag, Phys. Rev. Lett. **31**, 923 (1973).

[6]J. Ruvalds, J. Slinkman, A. K. Rajagopal, and A. Bagchi, Phys. Rev. B **16**, 2047 (1977); A. Bagchi and J. Ruvalds, Phys. Rev. A **8**, 1973 (1973).
[7]B. N. Esel'son, V. A. Slyusarev, V. I. Sobolev, and M. A. Strzhemechnyi, Zh. Eksp. Teor. Fiz. Pis'ma Red. **21**, 253 (1975).
[8]R. N. Bhatt, Phys. Rev. B **18**, 2108 (1978).
[9]W. Götze, M. Lücke, and A. Szprynger, Phys. Rev. B **19**, 206 (1979).
[10]We use the word spectrum for the Fourier transform of a correlation or response function, and the word dispersion for the wave-number dependence of a particular peak thereof.
[11]P. A. Hilton, R. Scherm, and W. G. Stirling, J. Low Temp. Phys. **27**, 851 (1977).
[12]D. S. Greywall, Phys. Rev. B **20**, 2643 (1979).
[13]R. B. Kummer, V. Narayanamurti, and R. C. Dynes, Phys. Rev. B **16**, 1046 (1977).
[14]D. L. Bartley, J. E. Robinson, and V. K. Wong, J. Low Temp. Phys. **12**, 71 (1973); D. L. Bartley, V. K. Wong, and J. E. Robinson, *ibid.* **17**, 551 (1974).
[15]M. Lücke and A. Szprynger, Phys. Rev. B **26**, 1374 (1982).
[16]J. M. Rowe, D. L. Price, and G. E. Ostrowski, Phys. Rev. Lett. **31**, 510 (1973).
[17]P. A. Hilton, W. G. Stirling, and R. Scherm (unpublished).
[18]K. S. Pedersen and R. A. Cowley, J. Phys. C **16**, 2671 (1983).
[19]D. L. Price, in *The Physics of Liquid and Solid Helium,* edited by K. H. Bennemann and J. B. Ketterson (Wiley, New York, 1978), Vol. II, p. 675.
[20]A. Fabrocini (unpublished).
[21]M. Suemitsu and Y. Sawada, Phys. Lett. **71A**, 71 (1979); Phys. Rev. B **25**, 4593 (1982).
[22]R. A. Cowley and A. D. B. Woods, Can. J. Phys. **49**, 177 (1970).
[23]D. S. Greywall, Phys. Rev. B **27**, 2747 (1983).
[24]C. H. Aldrich and d. Pines, J. Low Temp. Phys. **25**, 677 (1976); **32**, 689 (1978).
[25]H. R. Glyde and S. I. Hernadi, Phys. Rev. B **29**, 4926 (1984), and references cited therein.